Monthly Notices
of the
ROYAL ASTRONOMICAL SOCIETY

MNRAS **461,** 2809–2817 (2016)
Advance Access publication 2016 June 16

doi:10.1093/mnras/stw1442

A glitch in the millisecond pulsar J0613−0200

J. W. McKee,[1⋆] G. H. Janssen,[2⋆] B. W. Stappers,[1⋆] A. G. Lyne,[1] R. N. Caballero,[3] L. Lentati,[4] G. Desvignes,[3] A. Jessner,[3] C. A. Jordan,[1] R. Karuppusamy,[3] M. Kramer,[1,3] I. Cognard,[5,6] D. J. Champion,[3] E. Graikou,[3] P. Lazarus,[3] S. Osłowski,[3,7] D. Perrodin,[8] G. Shaifullah,[3,7] C. Tiburzi[3,7] and J. P. W. Verbiest[3,7]

[1]*Jodrell Bank Centre for Astrophysics, School of Physics and Astronomy, The University of Manchester, Manchester M13 9PL, UK*
[2]*ASTRON, the Netherlands Institute for Radio Astronomy, Postbus 2, NL-7990 AA, Dwingeloo, the Netherlands*
[3]*Max-Planck Institut für Radioastronomie, Auf dem Hügel 69, D-53121, Bonn, Germany*
[4]*Institute of Astronomy/Battcock Centre for Astrophysics, University of Cambridge, Madingley Road, Cambridge CB3 0HA, UK*
[5]*Laboratoire de Physique et Chimie de l'Environnement et de l'Espace LPC2E CNRS-Université d'Orléans, F-45071 Orléans, France*
[6]*Station de radioastronomie de Nançay, Observatoire de Paris, CNRS/INSU F-18330 Nançay, France*
[7]*Fakultät für Physik, Universität Bielefeld, Postfach 100131, D-33501 Bielefeld, Germany*
[8]*INAF – Osservatorio Astronomico di Cagliari, via della Scienza 5, I-09047 Selargius (CA), Italy*

Accepted 2016 June 13. Received 2016 May 26; in original form 2016 April 13

ABSTRACT

We present evidence for a small glitch in the spin evolution of the millisecond pulsar J0613−0200, using the EPTA Data Release 1.0, combined with Jodrell Bank analogue filterbank times of arrival (TOAs) recorded with the Lovell telescope and Effelsberg Pulsar Observing System TOAs. A spin frequency step of 0.82(3) nHz and frequency derivative step of $-1.6(39) \times 10^{-19}\,\mathrm{Hz\,s^{-1}}$ are measured at the epoch of MJD 50888(30). After PSR B1821−24A, this is only the second glitch ever observed in a millisecond pulsar, with a fractional size in frequency of $\Delta\nu/\nu = 2.5(1) \times 10^{-12}$, which is several times smaller than the previous smallest glitch. PSR J0613−0200 is used in gravitational wave searches with pulsar timing arrays, and is to date only the second such pulsar to have experienced a glitch in a combined 886 pulsar-years of observations. We find that accurately modelling the glitch does not impact the timing precision for pulsar timing array applications. We estimate that for the current set of millisecond pulsars included in the International Pulsar Timing Array, there is a probability of ∼50 per cent that another glitch will be observed in a timing array pulsar within 10 years.

Key words: stars: neutron – pulsars: general – pulsars: individual: PSR J0613−0200 – stars: rotation.

1 INTRODUCTION

Pulsars spin with remarkable stability, allowing pulse times of arrival (TOAs) to be accurately predicted with precisions, in the best cases, as high as fractions of microseconds over time-scales of decades. Millisecond pulsars (MSPs) in particular have such highly stable rotation that they are used as extremely precise clocks in timing experiments, and the most stable are used as probes of space–time in pulsar timing array (PTA) experiments. The ultimate goal is a direct gravitational wave (GW) detection in the nano-hertz regime (recent stochastic background limits are given in Arzoumanian et al. 2015, Lentati et al. 2015, Shannon et al. 2015). Since the influence of GWs on pulse TOAs is extremely small, the accuracy of the timing model describing the spin evolution of a pulsar needs to be very high in order to make a GW detection. This also requires the precise measurement and removal of other influences on the TOAs, such as those caused by changes in the interstellar medium (ISM) or irregularities in the pulsar spin evolution.

PSR J0613−0200 was discovered by Lorimer et al. (1995) and is a MSP which is included in all currently ongoing PTA experiments: the European Pulsar Timing Array (EPTA; Desvignes et al. 2016), the North American Nanohertz Observatory for Gravitational Waves (NANOGrav; Arzoumanian et al. 2015), the Parkes Pulsar Timing Array (PPTA; Reardon et al. 2016), and the International Pulsar Timing Array (IPTA; Verbiest et al. 2016). It has been timed to a precision of 1.2 μs over a time span of 13.7 years using the combined IPTA data set (Verbiest et al. 2016).

Although the spin evolution of pulsars is generally very stable and predictable, a small fraction of pulsars exhibit sudden

⋆ E-mail: james.mckee@manchester.ac.uk (JWM); janssen@astron.nl (GHJ); Ben.Stappers@manchester.ac.uk (BWS)

changes in spin frequency and/or frequency derivative, known as timing glitches. Timing glitches are usually associated with non-recycled and low-characteristic-age pulsars, notably the Crab pulsar (PSR B0531+21) and the Vela pulsar (PSR B0833−45), which have been observed to glitch 25 and 19 times, respectively, in 45 years of observations (Espinoza et al. 2011). Conversely, glitches in MSPs are exceedingly rare, with only one small glitch ever observed in the MSP B1821−24A (Cognard & Backer 2004), which is near the core of the globular cluster M28, and which displays significant timing noise (Fig. A1).

The mechanism which causes timing glitches is not fully understood, but is assumed to be linked to a sudden transfer of angular momentum from superfluid neutrons to the solid crust. The superfluid is thought to rotate independently from the rest of the neutron star and contains vortices. An ensemble of vortices becomes unpinned and a coupling to the solid component of the neutron star crust occurs, abruptly transferring angular momentum to it (a review of glitch models can be found in Haskell & Melatos 2015). The transfer of angular momentum generally increases the rotational frequency of the pulsar, which is occasionally observed to relax back to the pre-glitch value, although Archibald et al. (2013) have reported evidence for 'anti-glitches', a sudden *decrease* in the spin frequency in X-ray observations of the magnetar 1E 2259+586. The change in spin frequency and slowdown rate caused by a glitch are reflected in the deviation of the observed TOAs from the arrival times predicted by a pre-glitch timing model.

The glitch observed in PSR B1821−24A was notable as it was the first glitch to be observed in a MSP, and had a size $\Delta\nu/\nu = 8(1) \times 10^{-12}$, two orders of magnitude smaller than the next smallest glitch (at the time). The rarity of glitches in MSPs and the small size of the PSR B1821−24A glitch have led to speculation that MSPs have different structures to the rest of the population, or a different physical process could be responsible. Some proposed explanations are that PSR B1821−24A is a strange star, which experienced a crust-cracking event that would alter the angular momentum and cause the same effect on timing residuals as a small glitch (Mandal et al. 2006), or that the small size of the glitch is evidence of influence on the pulsar-term by a GW burst with memory (BWM), which could be indistinguishable from a post-glitch frequency step (Cordes & Jenet 2012).

Timing noise is a phenomenon where the observed arrival times of pulses deviate systematically from the timing solution through a process similar to a random walk in the spin parameters (e.g. Shannon & Cordes 2010). This manifests as structure in the timing residuals. Timing noise is thought to arise through unmodelled small-scale instabilities in the rotation of the pulsar. It has been shown that in slow pulsars, timing noise can be modelled as: a series of microglitches (Janssen & Stappers 2006), frequency derivative variations caused by magnetospheric switching (Lyne et al. 2010), or as post-glitch recovery stages (Hobbs, Lyne & Kramer 2010).

The structure for this paper is as follows: we describe our observations and data in Section 2, present our findings in Section 3, discuss the implications of our results in Section 4, and make closing conclusions in Section 5.

2 OBSERVATIONS

The data set comprises TOAs from a variety of pulsar backends used with the Lovell Telescope at Jodrell Bank in the UK, the Nançay Radio Telescope in France, the Effelsberg Radio Telescope in Germany, and the Westerbork Synthesis Radio Telescope in the Netherlands (Table 1). We have used the EPTA Data Release 1.0 (DR1; Desvignes et al. 2016) covering the time span MJD 50931−56795 and combined this with TOAs recorded using the Lovell telescope's analogue filterbank (AFB) backend for the epoch MJD 49030−55333, as well as some pre-DR1 Effelsberg TOAs using the Effelsberg-Berkeley pulsar processor (EBPP) backend and the Effelsberg Pulsar Observing System (EPOS). The TOAs and ephemeris for this pulsar will be made available on the EPTA webpage.[1]

The AFB and EPOS data were aligned with the DR1 data set using the default procedure of fitting constant phase offsets between the data sets at each observing frequency, as described in Desvignes et al. (2016). For a small subset of the AFB data at 1400 MHz, known hardware configuration changes were corrected for by adding a phase offset to the corresponding TOAs.

2.1 Jodrell bank analogue filterbank data

The AFB backend was used for pulsar observations with the Lovell telescope during the years 1982–2010. TOAs were derived from observations at centre frequencies of 400 MHz, 600 MHz, and 1400 MHz, and a time resolution of 250 μs (see Hobbs et al. 2004). Observations were hardware-dedispersed and average profiles were produced via pulse folding. Each TOA was generated through cross-correlation with an observing-frequency-specific template, and systematic offsets between different instruments and observing configurations were corrected for by fitting for constant offsets. The AFB data used a separate clock file for timing analysis (effectively treating the AFB as using a separate observatory to the digital filterbank used in more recent Lovell Telescope observations), as the AFB data had clock corrections already applied to the profiles, effectively absorbing the correction into the TOAs.

2.2 Effelsberg pulsar observing system

The EPOS backend (Jessner 1996) recorded observations using a 1390 MHz centre frequency, with a 40 MHz band split into sixty 666 kHz channels, which were digitally delayed (incoherently dedispersed) to correct for the DM of the pulsar. Observations were recorded at a time resolution of 60 μs, and folded using early Jodrell Bank timing models. The observations were time-stamped using a local hydrogen maser which was corrected to GPS. For more information on the EPOS system, see e.g. Kramer et al. (1998).

3 RESULTS

Combining the DR1 and earlier AFB TOAs revealed a sharp drift away from the DR1 timing solution, which was derived over the epoch MJD 50931 to 56795 (Fig. 1). Comparing the TOAs of pulsars timed to similar or better precision over the same time span did not show any similar drift. This rules out the possibility of an instrumental effect or an error in the clock corrections as the cause of the drift seen in the early data for PSR J0613−0200.

TOAs recorded using the Effelsberg EBPP backend in the epoch MJD 50362−50460 (i.e. preceding the start of DR1) and those from the EPOS backend were found to follow the same trend away from the predicted arrival time as the Lovell Telescope AFB data, excluding instrumental effects as the cause. ISM effects such as a steadily changing dispersion measure can also be ruled out,

[1] http://www.epta.eu.org/aom/

Table 1. PSR J0613−0200 timing data used in this study. The given rms refers to the solution *including* the fit for the glitch as presented in Table 2 when the MJD range covers the glitch epoch.

Telescope	Backend	Centre freq. (MHz)	$N_{\rm TOAs}$	MJD range	rms (μs)
Effelsberg	EPOS	1390	239	49768–51894	86.6
	EBPP	1360	46	54483–56486	1.5
	EBPP	1410	253	50362–54924	1.7
	EBPP	2638	72	53952–56486	6.1
Lovell	AFB	400	132	49030–50696	47.7
	AFB	600	142	49034–54632	22.3
	AFB	1400	586	49091–55333	18.3
	DFB	1400	24	54847–54987	5.4
	DFB	1520	191	55054–56760	2.0
NRT	BON	1400	334	53373–55850	1.1
	BON	1600	84	54836–56795	1.3
	BON	2000	51	54063–56224	2.3
WSRT	PUMA1	328	34	51770–55375	10.5
	PUMA1	382	27	51770–55375	8.0
	PUMA1	1380	99	51389–55375	3.0
Total	–	328–2638	2314	49030–56795	2.7

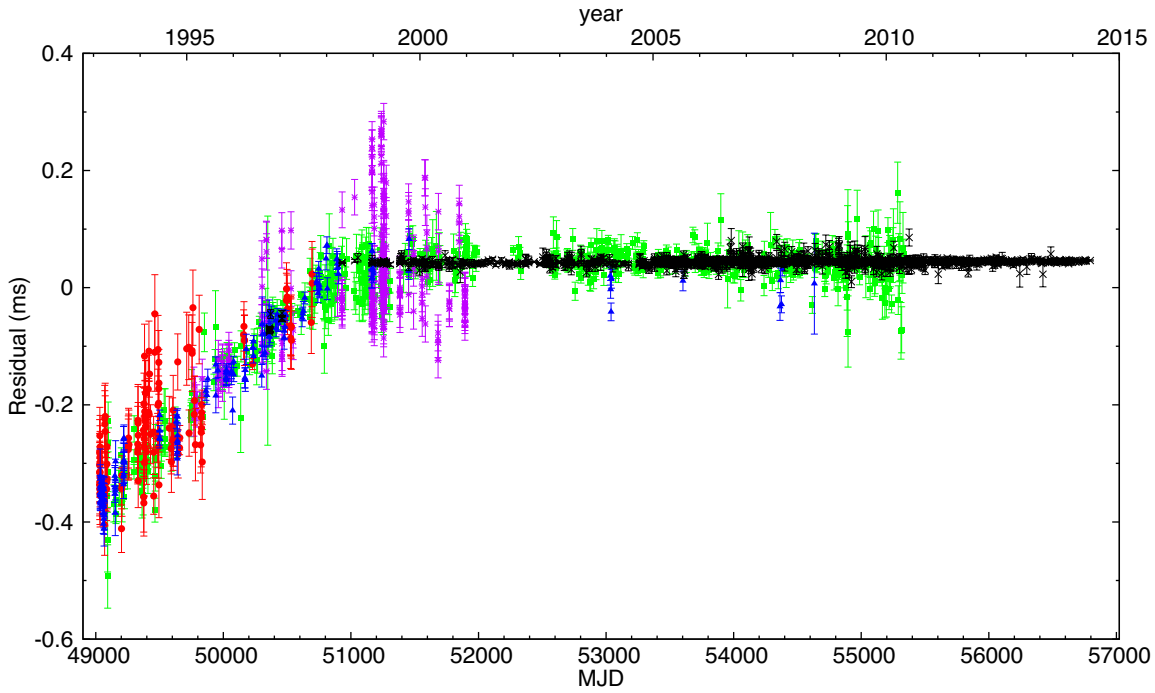

Figure 1. Timing residuals for PSR J0613−0200 (purple stars: EPOS 1390 MHz green squares: AFB 1400 MHz blue triangles: AFB 600 MHz red circles: AFB 400 MHz black crosses: DR1 including earlier EBPP 1410 MHz). TOAs were recorded using the instruments listed in Table 1, and analysed based on the EPTA Data Release 1.0 ephemeris. The timing solution does not accurately predict the arrival time of average pulses for dates earlier than the original EPTA data set (MJD 50931−56795) due to an unmodelled timing glitch occurring shortly before the epoch over which the EPTA ephemeris was derived.

as the effect is present and identical in data from three widely separated observing frequencies without showing any frequency-dependent trend which would be expected if the cause was ISM related.

The observed quasi-linear trend in the residuals is strong evidence of a timing glitch, and can be removed completely by fitting for glitch parameters not previously included in the timing solution, using a glitch epoch MJD 50888 (1998 March 16), which allows the pre-glitch and post-glitch frequency and frequency derivative to be derived (Table 2). Fitting for the spin parameters before and after the measured glitch epoch, we measure the fractional frequency step to be $\Delta\nu/\nu = 2.5(1) \times 10^{-12}$, and the fractional frequency derivative step to be $\Delta\dot{\nu}/\dot{\nu} = 1.6(39) \times 10^{-4}$, where here and elsewhere we use a 1σ uncertainty. The change in spin frequency over time was investigated by using a stride fit through our full data set, using a 500-d fitting window, and a step size of 100 d, which

Table 2. PSR J0613−0200 rotation parameters derived after fitting for the observed timing glitch, using the full EPTA Data Release 1.0 TOAs, pre-Data Release 1.0 EBPP 1410 MHz TOAs, EPOS 1390 MHz TOAs, and Jodrell Bank AFB 400–1400 MHz TOAs. Glitch parameters are estimated using our frequentist and Bayesian models described in the text.

Parameter	Frequentist value	Bayesian model (inc. sys. noise)	Bayesian model (no sys. noise)
Frequency epoch (MJD)	55 000	–	–
Frequency (Hz)	326.600 562 0227(2)	–	–
Frequency derivative (Hz s^{-1})	$-1.0228(4) \times 10^{-15}$	–	–
Glitch epoch (MJD)	50 888(30)	50 874(25)	50 922(14)
Glitch frequency step (Hz)	$8.2(3) \times 10^{-10}$	$8.7(6) \times 10^{-10}$	$7.6(3) \times 10^{-10}$
Glitch frequency derivative step (Hz s^{-1})	$-1.6(39) \times 10^{-19}$	$1.1(65) \times 10^{-19}$	$-1.2(4) \times 10^{-18}$

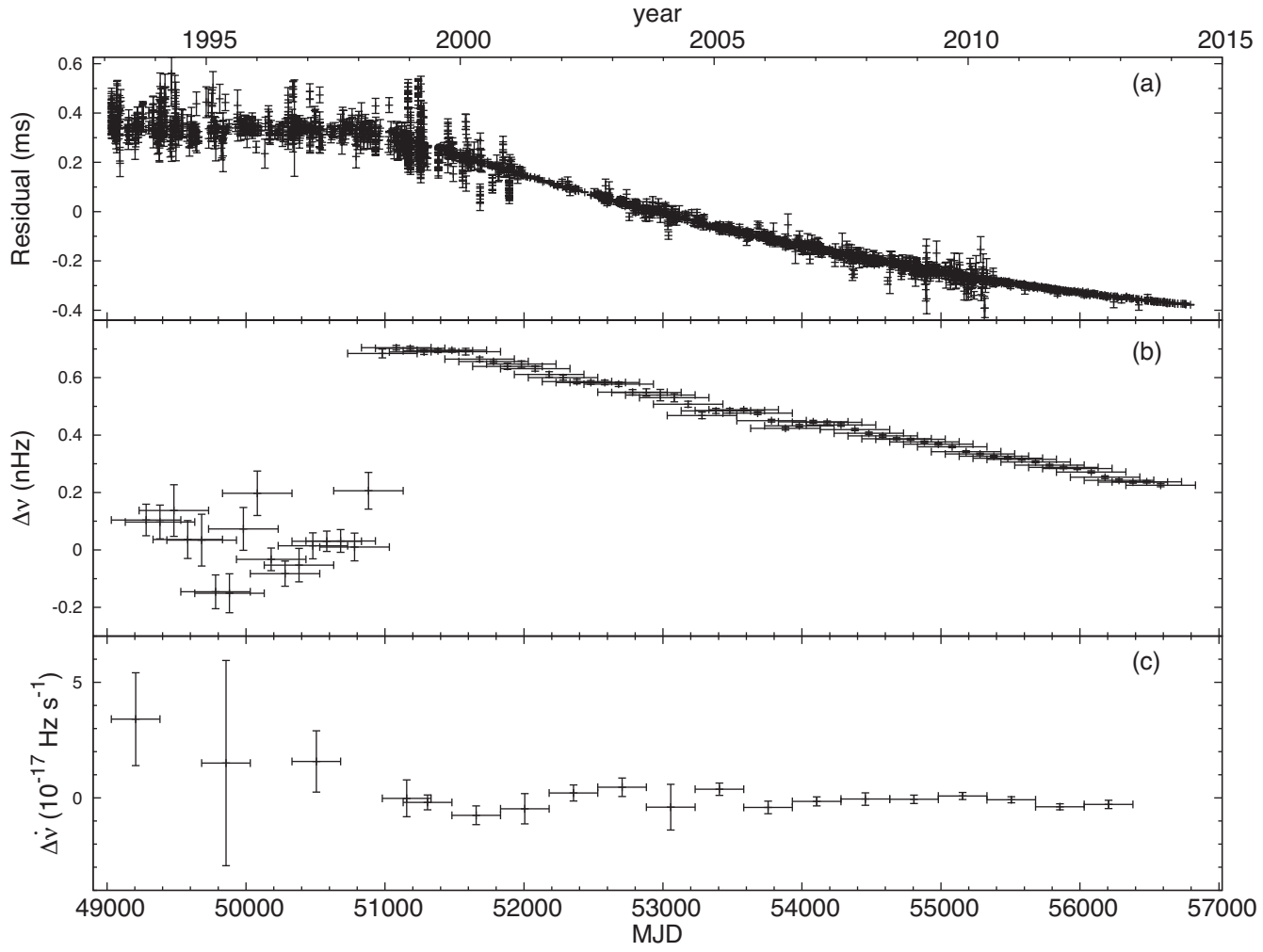

Figure 2. Rotational frequency evolution for PSR J0613−0200 from the pre-glitch ephemeris. (a) Timing residuals using a pre-glitch ephemeris, and our full data set described in Table 1. (b) Spin-frequency deviation from the ephemeris value derived using a stride fit through our full set of TOAs, using a 500-d window (represented by the horizontal error bars), and a 100-d stride length. (c) Frequency derivative variation from the ephemeris value over 350-d windows. The discontinuity is caused by the timing glitch occurring at MJD 50888(30) of fractional size $\Delta\nu/\nu = 2.5(1) \times 10^{-12}$, and the linear decrease by a change in frequency derivative of fractional size $\Delta\dot{\nu}/\dot{\nu} = -1.6(39) \times 10^{-4}$ (both values measured by fitting for pre-glitch and post-glitch spin parameters using the entire data set).

was necessary for deriving precise values for the spin frequency from the relatively large uncertainties in AFB and EPOS TOAs, while still allowing the sudden change in ν to be clearly identified (Fig. 2). The glitch epoch was estimated by fitting for all model parameters using TEMPO2 while varying the glitch epoch, and selecting the epoch corresponding to the minimum χ^2. The uncertainty in glitch epoch was taken as the region over which varying the epoch results in $\Delta\chi^2 = 1$. This is the smallest glitch ever recorded, with the next smallest also occurring in a MSP, with fractional frequency step $\Delta\nu/\nu = 8(1) \times 10^{-12}$ (Cognard & Backer 2004;

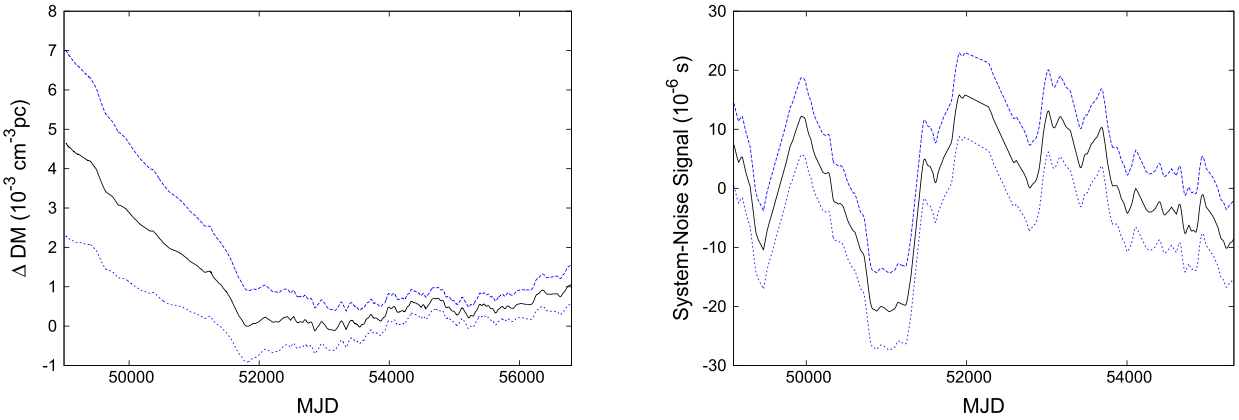

Figure 3. The mean value (black line) and 1σ confidence interval (blue lines) for DM variations (left panel), and system-dependent time-correlated noise in the AFB 1400 MHz data (right panel) assuming a power-law model for both processes.

Espinoza et al. 2011), i.e. several times larger than the glitch we report.

The possibility of a magnetospherically induced change in pulse shape related to a change in frequency derivative (Lyne et al. 2010) was considered as an alternative to a change in spin frequency, but no significant change of the pulse profile associated with the glitch was observed. However, it should be noted that the relatively low time resolution of the AFB and EPOS observations is insufficient for small pulse-shape changes to be detected. This effect was also tested for by fitting for separate frequency derivatives only (i.e. no change in spin frequency) for the pre-glitch and post-glitch residuals, using a range of epochs for the change in frequency derivative while keeping the rest of the parameters constant. The glitch signature was not effectively removed by this approach, with significant structure introduced to the timing residuals. To remove the glitch signature, a model that includes a step in spin frequency is required, therefore we rule out magnetospheric effects as an explanation for this event.

Following the EPTA timing and noise analysis in Desvignes et al. (2016) and Caballero et al. (2016), we use a Bayesian approach to confirm the findings of our frequentist analysis. We estimate the properties of the glitch simultaneously with different noise models using the Bayesian pulsar timing package TempoNest (Lentati et al. 2014). These noise models include parameters to modify the properties of the white noise, as well as time-correlated stochastic signals that describe DM variations, timing noise, and system-dependent noise. For this final term, we use the approach described in Lentati et al. (2016). For all noise models, we marginalize analytically over the full timing model while simultaneously searching for a glitch epoch, and changes in the spin frequency and frequency derivative at that epoch. We use priors that are uniform in the glitch parameters, where the glitch epoch is the full MJD range of the data set, and the glitch frequency and frequency derivative priors are uniform in amplitude. All Bayesian evidence comparisons thus do not assume a priori that a glitch is present in the data set.

We confirm the presence of a glitch, and find a model that includes both DM variations and additional system noise in the AFB 1400 MHz data set. We estimate a glitch epoch MJD 50874(25) from the system noise model, and MJD 50922(14) from the model without system noise. Using the system noise model, we estimate a spin-frequency step of 0.87(6) nHz and a spin-down rate step of $1.1(65) \times 10^{-19}\,\mathrm{Hz\,s^{-1}}$, and using the model with no system noise, we measure these quantities as 0.76(3) nHz and $-1.2(4) \times 10^{-18}\,\mathrm{Hz\,s^{-1}}$, respectively. In Fig. 3, we plot the mean signal realization with 1σ confidence intervals for the DM variations (top panel) and system noise (bottom panel) models. We find no evidence for a timing noise term that is coherent across all observing systems and is independent of the observing frequency ('spin noise' in Lentati et al. 2016). In principle, as we have only added additional observations to this data set compared to the DR1, we would expect that the sensitivity to timing noise would either be the same or improve relative to that analysis. However, the presence of significant system noise in the early AFB 1400 MHz data implies that the TOA estimates are affected by some time-correlated process that is potentially not well modelled by a stationary power-law noise process. If this early data were poorly modelled, then we would expect that including it in the data set would decrease our sensitivity to timing noise compared to DR1 as observed. We test the stationarity of this system noise term by including two additional parameters that define the start time and duration of noise process. We find that the evidence does not increase with the addition of these parameters, with the start time consistent with the beginning of the AFB 1400 MHz data set, and the duration consistent with the full length of the AFB 1400 MHz data, implying that this system noise is not the result of mismodelling the glitch or a temporary increase in the noise level of the data set. However, there is not a sufficient overlap of data to distinguish the system noise term in this data set, as explained in Lentati et al. (2016).

In Fig. 4, we show the one- and two-dimensional posterior probability distributions from our analysis for two different models. The black lines are from the optimal model that includes system noise, DM variations, and white noise parameters. The grey lines are from an analysis that includes DM variations and white noise parameters only in the stochastic model. We find the increase in the log evidence for the model that includes system noise is 24.7, which definitively supports their inclusion in the model. We confirm the detection of the glitch and find that the parameter estimates for the glitch model change significantly when including, or not, this additional system-dependent term. In particular, the uncertainties in the change in frequency and spin-down rate increase by a factor of 1.8, and the mean of the change in spin-down rate is consistent with zero at the $\sim 0.2\sigma$ level compared to the greater than 3σ detection in the model without system noise, but the

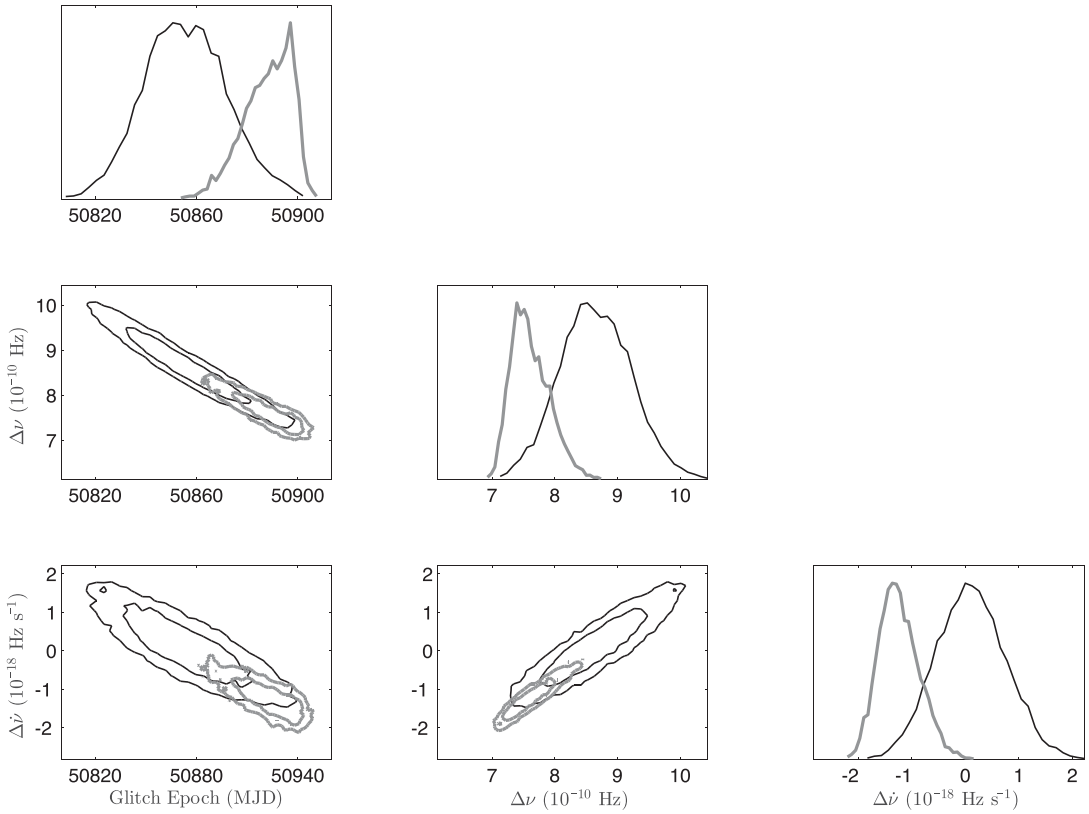

Figure 4. One- and two-dimensional posterior probability distributions for the glitch epoch, the change in spin frequency, and the change in spin-down rate for two different models for the stochastic properties of the data set, with 1 and 2σ confidence intervals shown in the contour plots. Grey lines: we include parameters that modify the properties of the white noise on a per system basis, scaling and adding in quadrature to the formal TOA uncertainties, and a power-law model for the DM variations. Black lines: we additionally include system-dependent time-correlated noise in the AFB 1400 MHz data. We find the change in the log evidence is 24.7 in favour of the more complex model, indicating definitive support for their inclusion.

results are consistent with the results of the frequentist approach presented in Table 2. We stress that with these results we do not claim that the model for system noise used in the analysis is the most optimal that could be used. However, it is significantly preferred by the data compared to a model that does not include it at all.

4 DISCUSSION

4.1 Pulsar timing array relevance

The detection prospects for GWs using a PTA rely on the timing of the pulsars included in the array to be extremely stable. Therefore, it may be reason for caution when a glitch is found in one of the most stable MSPs included in current PTA projects. However, our results show that the presence of a glitch in PSR J0613−0200 does not affect timing stability for PTA analysis, as TOAs used by the EPTA and IPTA for this pulsar are all derived using post-glitch observations. The occurrence of a glitch before the PTA epoch has not limited our ability to precisely time this pulsar. This is shown by statistical analyses of pulsar timing noise in PTAs, most recently by Caballero et al. (2016), in which red noise is only semi-defined for this pulsar. As the glitch is small and the red noise of the pulsar is not well-defined, it is therefore likely that potential unmodelled glitches outside the timing baseline for other PTA pulsars have no significant effect on timing array sensitivity.

Including this work, only two glitches have been reported in MSPs, and one in the recycled pulsar B1913+16 (Weisberg, Nice & Taylor 2010). Although small, the PSR J0613−0200 glitch was easy to detect with a data set covering a long baseline. We can therefore be confident that no other glitches with similar sizes have been missed in the spin-evolution of pulsars observed at Jodrell Bank Observatory (JBO). In this case, the effect of the glitch was easily removed without loss of timing precision, and so a glitch occurring in another PTA pulsar in the future may not be cause to remove the pulsar from future analysis. However, due to the unknown complexities of glitch models needed for MSPs, this is not completely certain. For future glitches in PTA pulsars, only the pre-glitch data would be usable until sufficient time had passed for the post-glitch spin parameters to be measured, or for any post-glitch pulse profile variation (Weltevrede, Johnston & Espinoza 2011; Keith, Shannon & Johnston 2013) to be recognized in the case of a magnetospheric variation.

4.2 MSP glitch rates

Following the discovery of the first MSP glitch, Cognard & Backer (2004) calculated an event rate of ∼1 glitch per 500 pulsar-years of combined observations (or ∼0.2 century^{-1}). A total of 105 MSPs (period $P < 10$ ms) are observed at JBO, with a combined total of 1118 pulsar-years observing time. This allows us to estimate an event rate of ∼1 glitch every 559 pulsar-years (or ∼0.18 century^{-1}), for glitches in MSPs of a size $\Delta\nu/\nu \gtrsim 2 \times 10^{-12}$, a rate

consistent with Cognard & Backer. We can extend this calculation to fully recycled pulsars by including PTA pulsars with $P > 10$ ms and some double neutron star binaries (where we choose an upper limit of $P \sim 59$ ms). We use this definition due to the difficulties in precisely defining recycled pulsars, but this allows us to estimate the order of magnitude of the glitch rate for this population. Following this, the glitch rate for recycled pulsars observed at JBO is $\sim$0.22 century^{-1}. We note that this rate is much lower than that for 'normal' pulsars of $\sim$1 glitch every 78 pulsar-years of observation (or $\sim$1.3 century^{-1}). At JBO, 42 of the 49 IPTA pulsars (Verbiest et al. 2016) have been observed for a combined total of 793 pulsar-years, while the other seven have 93.5 pulsar-years of observations in the IPTA data release. This gives a combined total of 886 pulsar-years, in which time only two glitches have been observed (a rate of $\sim$0.23 century^{-1}). If we assume this is a good approximation of the PTA glitch return rate r pulsar-years, then the probability of a glitch occurring in t years is $P = 1 - (1 - r^{-1})^t$. For observations of the 49 pulsars in the IPTA, this gives a probability of $\sim$70 per cent that another glitch will be observed in a PTA in the next 10 years, and $\sim$95 per cent that a glitch will be observed in the next 27 years. If we exclude PSR B1821−24A from the analysis, due to its unusual timing noise and acceleration within the host globular cluster, the return rate is $\sim$0.12 century^{-1}, with an $\sim$50 per cent probability of a glitch in the next 10 years, and $\sim$95 per cent in the next $\sim$50 years. As discussed earlier, the clear detection of such a small glitch in relatively low-precision data suggests that no such glitches have avoided detection in similarly precisely timed MSPs.

It should be noted that the event rates calculated here assume that all MSPs and recycled pulsars are equally likely to experience a glitch, and that the probability remains the same following a glitch. This is probably not true, as the internal structure of the neutron stars is an important factor in the true glitch rate. The calculated glitch rates are therefore only estimates, but allow us to consider how likely it is that a glitch will occur in a 10 + year data set required for a GW detection. There are also biases in our calculations which would need to be addressed for the true rates to be obtained. For example, we are biased against glitches occurring very early or late in a data set, due to the difficulty in recognizing their effect.

4.3 Neutron star structure

The discovery of a glitch in PSR B1821−24A led to speculation on the nature of neutron star structure, due to the small size of the glitch, the high rotation frequency of the pulsar, and the relatively low magnetic field strength (2.25×10^9 G) compared to other glitching pulsars ($\gtrsim 10^{11}$ G). Mandal et al. (2009) interpreted this as evidence for PSR B1821−24A being a strange star due to the magnitude of the observed glitch being consistent with the modelled values arising from a cracking of the strange star crust. By comparison, we derive the inferred surface magnetic field strength of PSR J0613−0200 from the period and spin-down rate to be 1.7×10^8 G, an order of magnitude lower than that of PSR B1821−24A. Mandal et al. (2009) also noted that the PSR B1821−24A glitch energy budget $\Delta E \sim 10^{40}$ erg, given by $\Delta E = \delta(I\nu^2) \sim I\nu^2(\frac{\delta\nu}{\nu}) \sim E_{\rm rot}(\frac{\delta\nu}{\nu})$, stood out from the rest of the population, which follow a line on a log ΔE versus log $\Delta\nu/\nu$ plot, when assuming all neutron stars have the same moment of inertia $I = 10^{45}$ g cm^{-2}. This implies that the large amount of energy required for such a change in angular momentum may not be readily available to MSPs. The PSR J0613−0200 energy budget $\Delta E \sim 2 \times 10^{39}$ erg also does not follow the same distribution. It is therefore apparent that the combination of small glitch sizes, greater characteristic ages (30 Myr and 5 Gyr for PSR B1821−24A and PSR J0613−0200, respectively), lower magnetic field strengths, and energy budgets imply that while MSPs are most likely neutron stars (e.g. recent MSP mass measurements in Antoniadis et al. 2016), they could potentially have a different interior structure to the rest of the population, which may cause the glitch mechanism or properties to be different. The uniqueness of the three glitching recycled pulsars can be seen in the P–$\dot{P}$ diagram (Fig. A1).

4.4 Gravitational wave memory

One of the proposed causes of a GW signal in PTA data is a BWM, caused by a merger of a supermassive black hole binary (SMBHB), which will leave a lasting change (offset) in space–time (Braginskii & Thorne 1987). The main signature of such a burst in pulsar TOAs is a step in frequency, without a step in frequency derivative. When a BWM passes over the Earth, a step will be seen at the same time in all pulsars that are observed (Earth term). However, since the signal travels at the speed of light, when a BWM passes over a pulsar, it will not be seen in other pulsars in the PTA at the same time, due to the large light travel time between pulsars. If a BWM affects only the pulsar term, this could be difficult to distinguish from a glitch, as only a single pulsar is affected. There will also be no exponential recovery, as seen for some glitches (Cordes & Jenet 2012). This would be difficult to identify in PSR J0613−0200, as Lyne, Pritchard & Shemar (1995) noted the percentage glitch recovery decreases with characteristic age of the pulsar, making it effectively zero for a 5 Gyr characteristic age. Madison, Cordes & Chatterjee (2014) compare the BWM effect with the size of the glitch in PSR B1821−24A. They conclude that if the frequency change in that pulsar would have been caused by a BWM instead of a glitch, this would have required an impossible scenario of a merger of a $\sim 10^{10} M_\odot$ edge-on SMBHB only 10 Mpc from the Milky Way. Such a system is excluded by single-source GW limits (see e.g. Yi et al. 2014; Dolch et al. 2014; Babak et al. 2016).

We use the same argument to rule out a BWM scenario for the signature in our data on PSR J0613−0200. Although the change in spin-down rate is consistent with zero, the glitch size is too large to make a BWM a realistic scenario for our measurements.

5 CONCLUSIONS

We have measured a spin frequency step in PSR J0613−0200 that we attribute to a small glitch, making this only the second detection of a glitch in a MSP, and the smallest glitch size recorded to date. We rule out other possibilities, such as magnetospherically induced variations in rotation and pulse shape, and a GW BWM, due to the absence of effects associated with these causes. We interpret the difference between glitches in MSPs and the general pulsar population as potential indications of differences in MSP interior structure, and find that the glitch rate for MSPs is significantly different from that of the general population. We demonstrate that glitch events are rare in PTA pulsars. Although their effect on the TOAs is significant, they can be accounted for without any further consequences for GW experiments when sufficient post-glitch timing data are available to correct for the glitch signature.

ACKNOWLEDGEMENTS

We thank L. Levin for useful discussions. The authors acknowledge the support of the colleagues in The European Pulsar Timing Array.

The EPTA is a collaboration between European institutes, namely ASTRON (NL), INAF/Osservatorio di Cagliari (IT), Max Planck Institut für Radioastronomie (GER), Nançay/Paris Observatory (FRA), University of Leiden (NL) and the University of Manchester (UK), with the aim to provide high precision pulsar timing to work towards the direct detection of low-frequency GWs. An Advanced Grant of the European Research Council to implement the Large European Array for Pulsars (LEAP) also provides funding.

Part of this work is based on observations with the 100-m telescope of the Max-Planck-Institut für Radioastronomie (MPIfR) at Effelsberg. Access to the Lovell Telescope is supported through an STFC consolidated grant. The Nançay radio telescope is part of the Paris Observatory, associated with the Centre National de la Recherche Scientifique (CNRS), and partially supported by the Région Centre in France. The Westerbork Synthesis Radio Telescope is operated by the Netherlands Institute for Radio Astronomy (ASTRON) with support from The Netherlands Foundation for Scientific Research NWO.

SO is supported by the Alexander von Humboldt Foundation. PL gratefully acknowledges financial support by the European Research Council for the ERC Starting Grant BEACON under contract no. 279702.

This work was supported by the UK Science and Technology Research Council, under grant number ST/L000768/1

REFERENCES

Antoniadis J., Tauris T. M., Ozel F., Barr E., Champion D. J., Freire P. C. C., 2016, ApJ, preprint, (arXiv:1605.01665)
Archibald R. F. et al., 2013, Nature, 497, 591
Arzoumanian Z. et al., 2015, ApJ, 813, 65
Babak S. et al., 2016, MNRAS, 455, 1665
Braginskii V. B., Thorne K. S., 1987, Nature, 327, 123
Caballero R. N. et al., 2016, MNRAS, 457, 4421
Cognard I., Backer D. C., 2004, ApJ, 612, L125
Cordes J. M., Jenet F. A., 2012, ApJ, 752, 54
Desvignes G. et al., 2016, MNRAS, 458, 3341
Dolch T. et al., 2014, ApJ, 794, 21
Espinoza C. M., Lyne A. G., Stappers B. W., Kramer M., 2011, MNRAS, 414, 1679
Haskell B., Melatos A., 2015, Int. J. Modern Phys. D, 24, 1530008
Hobbs G., Lyne A. G., Kramer M., Martin C. E., Jordan C., 2004, MNRAS, 353, 1311
Hobbs G., Lyne A. G., Kramer M., 2010, MNRAS, 402, 1027
Janssen G. H., Stappers B. W., 2006, A&A, 457, 611
Jessner A., 1996, in van't Klooster C. G. M., van Ardenne A., eds, Large Antennas in Radio Astronomy. ESTEC, Noordwijk, p. 185
Keith M. J., Shannon R. M., Johnston S., 2013, MNRAS, 432, 3080
Kramer M., Xilouris K. M., Lorimer D. R., Doroshenko O., Jessner A., Wielebinski R., Wolszczan A., Camilo F., 1998, ApJ, 501, 270
Lentati L., Alexander P., Hobson M. P., Feroz F., van Haasteren R., Lee K. J., Shannon R. M., 2014, MNRAS, 437, 3004
Lentati L. et al., 2015, MNRAS, 453, 2576
Lentati L. et al., 2016, MNRAS, 458, 2161
Lorimer D. R. et al., 1995, ApJ, 439, 933
Lyne A. G., Pritchard R. S., Shemar S. L., 1995, JA&A, 16, 179
Lyne A., Hobbs G., Kramer M., Stairs I., Stappers B., 2010, Science, 329, 408
Madison D. R., Cordes J. M., Chatterjee S., 2014, ApJ, 788, 141
Mandal R. D. R., Sinha M., Bagchi M., Konar S., Dey M., Dey J., 2006, MNRAS, 365, 1383
Mandal R. D. R., Konar S., Dey M., Dey J., 2009, MNRAS, 399, 822
Reardon D. J. et al., 2016, MNRAS, 455, 1751
Shannon R. M., Cordes J. M., 2010, ApJ, 725, 1607
Shannon R. M. et al., 2015, Science, 349, 1522
Verbiest J. P. W. et al., 2016, MNRAS, 458, 1267
Weisberg J. M., Nice D. J., Taylor J. H., 2010, ApJ, 722, 1030
Weltevrede P., Johnston S., Espinoza C. M., 2011, MNRAS, 411, 1917
Yi S., Stappers B. W., Sanidas S. A., Bassa C. G., Janssen G. H., Lyne A. G., Kramer M., Zhang S.-N., 2014, MNRAS, 445, 1245

APPENDIX: P–$\dot{P}$ DIAGRAM

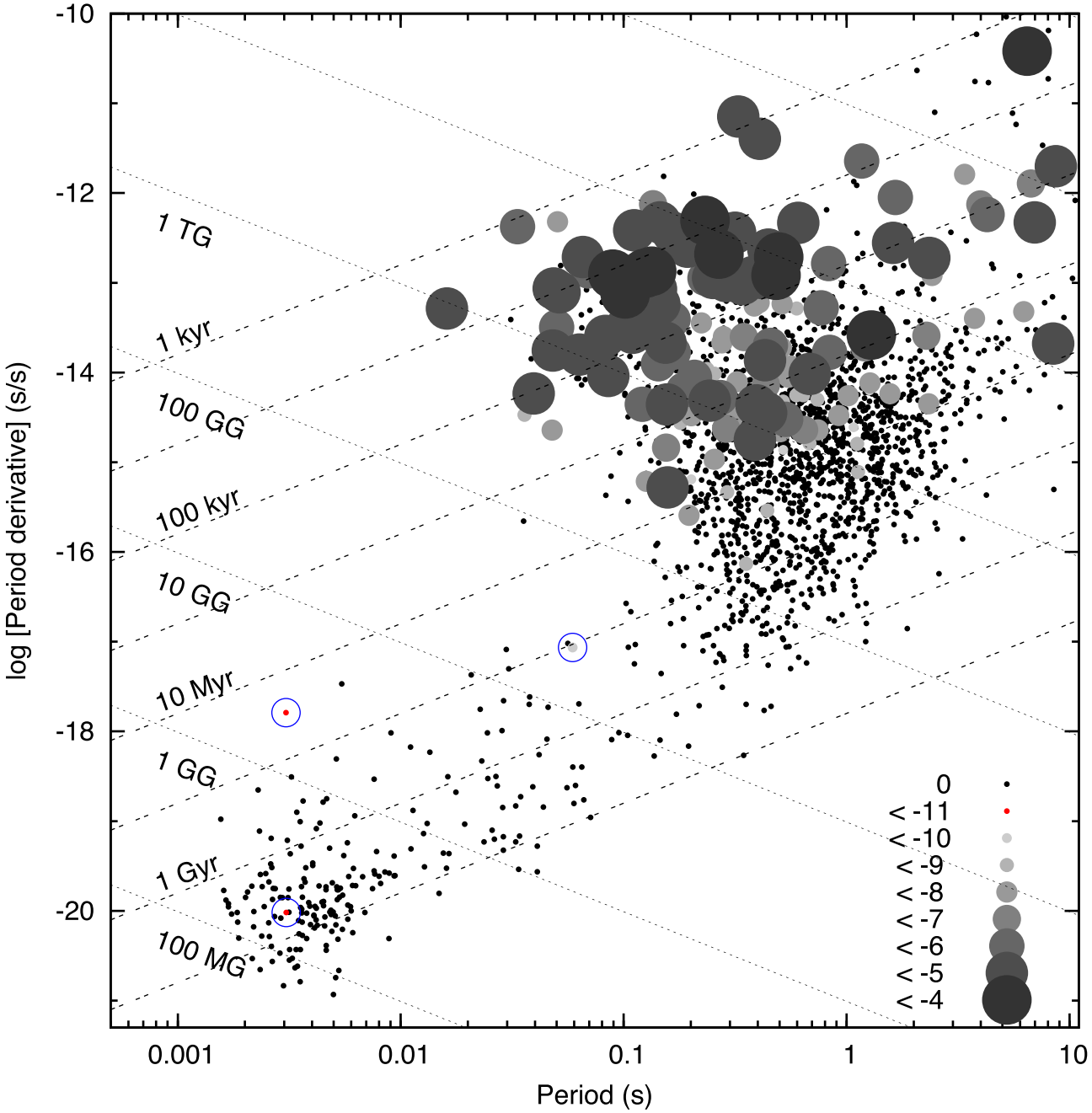

Figure A1. P–$\dot{P}$ diagram with pulsars labelled according to their cumulative spin frequency change due to glitches, $\log[\Sigma\,\Delta\nu/\nu]$. The labels in the key are the upper limit of the glitch size bins, which are in intervals of one order of magnitude. The three recycled pulsars for which a glitch has been observed are circled: B1913+16 (59 ms, 8.6×10^{-18} s s^{-1}), B1821−24A (3 ms, 1.6×10^{-18} s s^{-1}), and J0613−0200 (3 ms, 9.6×10^{-21} s s^{-1}). The uniqueness of the PSR J0613−0200 glitch is apparent, due to its small size, and the location of J0613−0200 in the middle of the MSP 'island'.

This paper has been typeset from a TEX/LATEX file prepared by the author.